Managing RES Uncertainty and Stability Issues in Distribution Systems via Energy Storage Systems and Switchable Reactive Power Sources

Mário P.S. Pereira[1], D.Z. Fitiwi[2], S.F. Santos[2], J.P.S Catalão[1,2,3]
INESC TEC and FEUP[1], Porto, C-MAST/UBI[2], Covilhã, INESC-ID/IST-UL[3], Lisbon, Portugal
mp0721@gmail.com; dzf@ubi.pt; sdfsantos@gmail.com; catalao@fe.up.pt

***Abstract*—In the last decade, the level of variable renewable energy sources (RESs) integrated in distribution network systems have been continuously growing. This adds more uncertainty to the system, which also faces all traditional sources of uncertainty and those pertaining to other emerging technologies such as demand response and electric vehicles. As a result, distribution system operators are finding it increasingly difficult to maintain an optimal daily operation of such systems. Such challenges/limitations are expected to be alleviated when distribution systems undergo the transformation process to smart grids, equipped with appropriate technologies such as energy storage systems (ESSs) and switchable capacitor banks (SCBs). These technologies offer more flexibility in the system, allowing effective management of the uncertainty in RESs. This paper presents a stochastic mixed integer linear programming (SMILP) model, aiming to optimally operate distribution network systems, featuring variable renewables, and minimizing the impact of RES uncertainty on the system's overall performance via ESSs and SCBs. A standard 41-bus distribution system is employed to show the effectiveness of the proposed S-MILP model. Simulation results indicate that strategically placed ESSs and SCBs can substantially alleviate the negative impact of RES uncertainty in the considered system.**

NOMENCLATURE

A. Sets/Indices

i/Ω^i	Index/set of buses
$g/\Omega^g/\Omega^{DG}$	Index/set of generators/DGs
l/Ω^l	Index/set of branches
s/Ω^s	Index/set of scenarios
h/Ω^h	Index/set of hours
cb/Ω^{cb}	Index/set of capacitor banks
ζ/Ω^{ζ}	Index/set of substations
y	Index of linear segments

B. Parameters

$E^{min}_{es,i}, E^{max}_{es,i}$	Energy storage limits (MWh)
ER_g, ER_{SS}	Emission rates of DGs and energy purchase upstream, respectively (tCO_2e/MWh)
g_l, b_l, S^{max}_l	Conductance, susceptance and flow limit of branch *l*, respectively ($\mho, \mho$ MVA)
$OC_{g,i,s,h}$	Operation cost of DGs (€/MWh)
pf_g	DG power factor
pf_{ss}	Power factor at substation
$Q^{cb,\,max}_i$	Maximum capacitor bank capacity at node *i* (MVAr)
r_l, x_l	Resistance and reactance of branch *l*, respectively (Ω, Ω)
$u_{es,i,h}$	Utilization status of storage system (1 if connected, 0 otherwise)
V_{nom}	Nominal voltage (kV)
$v_{s,h}$	Penalty for unserved power (€/MW)
Y	Total number of linear segments
$\alpha_{l,y}, \beta_{l,y}$	Slopes of linear segments *y* of branch *l*
$\eta^{ch}_{es}, \eta^{dch}_{es}$	Charging and discharging efficiencies of storage systems (%)
$\Delta V^{min}, \Delta V^{max}$	Limits for voltage deviations (kV)
$\lambda^{\zeta}_{s,h}$	Price of electricity purchased from upstream (€/MWh)
$\lambda^{CO2}_{s,h}$	Price of emissions (€/tCO_2e)
ρ_s	Probability of scenario *s*

C. Variables

CET	Total cost of emissions (expected)
COT	Total operation cost (expected)
CUT	Total cost of unserved power (expected)
TC	Total cost (objective function)
$DemP^i_{s,h}$	Active power demand at node *i* (MW)
$DemQ^i_{s,h}$	Reactive power demand at node *i* (MVAr)
$E_{es,i,s,h}$	Stored energy (MWh)
$I^{ch}_{es,i,h}, I^{dch}_{es,i,h}$	Charge and discharge indicator variables, respectively
$P^{SS}_{\zeta,s,h}, Q^{SS}_{\zeta,s,h}$	Active and reactive power import from grid (MW, MVAr)
$P^{ch}_{es,i,s,h}, P^{dch}_{es,i,s,h}$	Charged and discharged power (MW)
$P_{g,i,s,h}$	Active power produced by DGs (MW)
$P^{un}_{i,s,h}, Q^{un}_{i,s,h}$	Active and reactive power unserved at *i* (MW, MVAr)

This work was supported by FEDER funds through COMPETE 2020 and by Portuguese funds through FCT, under Projects SAICT-PAC/0004/2015 - POCI-01-0145-FEDER-016434, POCI-01-0145-FEDER-006961, UID/EEA/50014/2013, UID/CEC/50021/2013, and UID/EMS/00151/2013. Also, the research leading to these results has received funding from the EU Seventh Framework Programme FP7/2007-2013 under grant agreement no. 309048.

978-1-5386-3917-7/17/$31.00 © 2017 IEEE

$p_{l,s,h,y}, q_{l,s,h,y}$	Step variables used to linearize the quadratic flows (MW, MVAr)
P_l, Q_l, θ_l	Active and reactive power flows, and voltage angle difference of branch *l*, respectively (MW, MVAr, radians)
$PL_{l,s,h}, QL_{l,s,h}$	Active and reactive power losses of branch *l* (MW, MVAr)
$Q_{g,i,s,h}$	Active power produced/consumed by DGs (MVAr)
$Q^{cb}_{i,s,h}$	Reactive power injected at node *i* by capacitor bank (MVAr)
$V_{i,s,h}, V_{j,s,h}$	Voltage magnitudes of node *i* and *j* within the same branch (kV)
$\theta_{i,s,h}, \theta_{j,s,h}$	Voltage angles at node *i* and *j* within the same branch (radians)
$\lambda^{dch}_{s,h}$	Cost of storage system (€/MWh)

I. Introduction

Power systems have experienced significant changes in the last decade. In particular, distribution network systems are now gradually evolving from passive to active network systems. These changes are as a result of the need for the energy systems to adapt to new challenges such as the continuous increase in demand for electricity [1], environmental concerns associated with conventional power generation practices, energy transmission and distribution, etc. In order to partly overcome such challenges, distributed generation (DG) systems (renewables, in particular) have been integrated in the energy systems, which is becoming a common practice throught the world.

However, the integration of variable renewable energy sources (RESs) comes with several challenges, both economic and technical. On the technical side, the first major challenge that immediately comes with RES integration is related to the uncertainty and variability of renewables, which "make the management of network systems very difficult" [2]. Furthermore, violations of system-wide technical restrictions are not tolerated especially at distribution levels, that is, the system should always operate respecting the technical limitations [3]. On the economical point of view, the non-dispatchable nature of RES, especially wind and solar, brings additional costs. To overcome these challenges several countries are investing in planning and expanding their current infrastructure to cope with RES integration [4]. It is necessary to introduce technologies that facilitate the integration of variable RESs and their effective management. Among others, the optimal use of energy storage systems (ESSs) and switchable capacitor banks (SCBs) is a viable option capable of addressing the aforementioned challenges, at least partly.

It is now widely accepted that ESSs will be extremely important components of future power systems because they help to counteract the unpredictable variation of the energy generated using RESs, as well as the uncertainty associated with power supply, which adversely affects the optimal operation and reliability of the traditional electrical systems [5]. Therefore, the use of ESSs allows to level the incompatibility between energy generation and demand [6], [7]. In addition, ESSs can contribute to relieving the fluctuation of power from RESs, low voltage ride through, and voltage support, resulting in smoother system operations. In [8], the wide-range benefits of using ESSs in the distribution system are extensively discussed. Despite all this, ESSs are yet very expensive. However, with the continuous technological development, the cost of most ESS technologies has been decreasing with high learning rates. A recent study on cost-benefit analysis of ESSs has shown that ESSs are becoming increasingly competitive, and the use of such technologies is justified in many cases [8].

Another relatively cheaper technology that allows greater integration and management of RESs is switchable capacitor bank. This is due to the fact that power systems require a significant amount of reactive power to maintain the voltage in the nodes within specified ranges. There are several switching methods such as the VAR compensation source but the most commonly used is switchable capacitor banks since capacitors are passive filters and do not interfere with the optimization process [9]. Therefore, capacitor banks are widely used as effective technologies, both at the transmission and distribution levels. In addition to maintaining the nodal voltages at standard levels, capacitor banks can be used to reduce energy losses by injecting reactive power into substations [10], thereby increasing system capacity and correcting system power factor [11]. Capacitor banks placement along the line will compensate for the inductive or reactance's loads of the lines [12]. In the literature, several capacitor bank positioning techniques have been proposed as in [10], [13]–[15].

This work develops a new stochastic MILP model that aims to ensure a more efficient utilization of variable renewables at distribution levels. In addition, the model is used for managing the uncertainty inherent to such energy sources with properly located ESSs and SCBs, thereby maintaining the stability and the integrity of distribution networks systems as well as the power quality in the system.

II. Mathematical Formulation

A. Objective Function

As described in [16], the location of the different resources is already predetermined. The objective of this work is to investigate an optimal operation of distribution grids featuring large-scale RES based DGs, SCBs and ESSs, in order to cope with the variability of wind and solar power production.

The objective function minimizes the sum of expected costs of operation, emission, unserved energy and emissions along the optimization scope.

$$MinTC = COT + CUT + CET \tag{1}$$

The total operation cost is given by the sum of expected costs of power generation by DGs, import power and discharged power as:

$$
\begin{aligned}
COT = & \sum_{s\in\Omega^s} \rho_s * \sum_{h\in\Omega^h} \sum_{g\in\Omega^g} \sum_{i\in\Omega^i} OC_{g,i,s,h} * P_{g,i,s,h} \\
& + \sum_{s\in\Omega^s} \rho_s * \sum_{h\in\Omega^h} \sum_{\zeta\in\Omega^\zeta} \lambda^{\zeta}_{s,h} * P^{SS}_{\zeta,s,h} \\
& + \sum_{s\in\Omega^s} \rho_s * \sum_{h\in\Omega^h} \sum_{es\in\Omega^{es}} \sum_{i\in\Omega^i} \lambda^{dch}_{s,h} * P^{dch}_{es,i,s,h}
\end{aligned} \tag{2}
$$

Cost of discharge is considered to account for the degradation of the energy storage system.

To model the total cost of unserved power cost, a penalty ($v_{s,h}$) is considered:

$$
CUT = \sum_{s\in\Omega^s} \rho_s * \sum_{h\in\Omega^h} \sum_{i\in\Omega^i} v_{s,h} * (P^{un}_{i,s,h} + Q^{un}_{i,s,h}) \tag{3}
$$

The final equation that is part of the objective function refers to the total cost of emissions. It is modeled as:

$$
\begin{aligned}
CET = & \sum_{s\in\Omega^s} \rho_s * \sum_{h\in\Omega^h} \sum_{g\in\Omega^g} \sum_{i\in\Omega^i} \lambda^{CO2}_{s,h} * ER_g * P_{g,i,s,h} \\
& + \sum_{s\in\Omega^s} \rho_s * \sum_{h\in\Omega^h} \sum_{\zeta\in\Omega^\zeta} \lambda^{CO2}_{s,h} * ER_{SS} * P^{SS}_{\zeta,s,h}
\end{aligned} \tag{4}
$$

B. Constraints

For computation reasons, the non-linear and non-convex AC power flow equations are often linearized under various simplifying assumptions. Here, the linearized AC network model proposed in [17] is being considered. The linearized active and reactive power flow constraints are:

$$
P_{l,s,h} \approx V_{nom}(\Delta V_{i,s,h} - \Delta V_{j,s,h}) g_l - V^2_{nom} b_l(\theta_{l,s,h}) \tag{5}
$$

$$
Q_{l,s,h} \approx -V_{nom}(\Delta V_{i,s,h} - \Delta V_{j,s,h}) b_l - V^2_{nom} g_l(\theta_{l,s,h}) \tag{6}
$$

The thermal limit in a feeder is given by:

$$
P^2_{l,s,h} + Q^2_{l,s,h} \leq (S^{max}_l)^2 \tag{7}
$$

The quadratic expression (7) is linearized using a piecewise linearization, considering a sufficient number of linear segments, *Y*. In this study, *Y* is considered equal to 5, a number which balances accuracy with computation burden [18]. There are several ways of linearizing such functions as described in [19]. This approach is based on a first-order approximation of a non-linear curve, and is chosen due to its relatively simple formulation. In order to reduce the mathematical complexity of the formulation, two non-negative auxiliary variables are introduced for each of the flows P_l and Q_l, where $P_l = P^+_l - P^-_l$ and $Q_l = Q^+_l - Q^-_l$. These auxiliary variables (P^+_l, P^-_l, Q^+_l and Q^-_l) represent the positive and negative flows of P_l and Q_l, respectively.

The associated constraints, in this case, are presented below:

$$
P^2_{l,s,h} \approx \sum_{y=1}^{Y} \alpha_{l,y} p_{l,s,h,y} \tag{8}
$$

$$
Q^2_{l,s,h} \approx \sum_{y=1}^{Y} \beta_{l,y} q_{l,s,h,y} \tag{9}
$$

$$
P^+_{l,s,h} + P^-_{l,s,h} = \sum_{y=1}^{Y} p_{l,s,h,y} \tag{10}
$$

$$
Q^+_{l,s,h} + Q^-_{l,s,h} = \sum_{y=1}^{Y} q_{l,s,h,y} \tag{11}
$$

where $p_{l,s,h,y} \leq S^{max}_l / Y$ and $q_{l,s,h,y} \leq S^{max}_l / Y$.

The active and reactive power losses in line l can be approximated as:

$$
PL_{l,s,h} = r_l (P^2_{l,s,h} + Q^2_{l,s,h}) / V^2_{nom} \tag{12}
$$

$$
QL_{l,s,h} = x_l (P^2_{l,s,h} + Q^2_{l,s,h}) / V^2_{nom} \tag{13}
$$

The details related to (12) and (13) can be found in [17].

To ensure that, at all time, load balances are respected, the sum of of all injections should be equal to the sum of all withdrawals at each node for both active (14) and reactive (15) loads, which is *Kirchhoff's Current Law*:

$$
\begin{aligned}
& P^{SS}_{\zeta,s,h} + \sum_{g\in\Omega^{DG}} P_{g,i,s,h} + \sum_{es\in\Omega^{es}} (P^{dch}_{es,i,s,h} - P^{ch}_{es,i,s,h}) \\
& + \sum_{in,l\in i} P_{l,s,h} - \sum_{out,l\in i} P_{l,s,h} + P^{un}_{i,s,h} \\
& = Dem P^i_{s,h} + \sum_{in,l\in i} \frac{1}{2} PL_{l,s,h} + \sum_{out,l\in i} \frac{1}{2} PL_{l,s,h} \; \forall \; \zeta \in i
\end{aligned} \tag{14}
$$

$$
\begin{aligned}
& Q^{SS}_{\zeta,s,h} + \sum_{g\in\Omega^{DG}} Q_{g,i,s,h} + \sum_{cb\in\Omega^{cb}} Q^{cb}_{i,s,h} \\
& + \sum_{in,l\in i} Q_{l,s,h} - \sum_{out,l\in i} Q_{l,s,h} \\
& = Dem Q^i_{s,h} + \sum_{in,l\in i} \frac{1}{2} QL_{l,s,h} + \sum_{out,l\in i} \frac{1}{2} QL_{l,s,h} \; \forall \; \zeta \in i
\end{aligned} \tag{15}
$$

ESS constraints are presented below:

$$
0 \leq P^{ch}_{es,i,s,h} \leq u_{es,i,h} I^{ch}_{es,i,h} P^{ch,max}_{es,i,s,h} \tag{16}
$$

$$
0 \leq P^{dch}_{es,i,s,h} \leq u_{es,i,h} I^{dch}_{es,i,h} P^{dch,max}_{es,i,s,h} \tag{17}
$$

$$
I^{ch}_{es,i,h} + I^{ch}_{es,i,h} \leq 1 \tag{18}
$$

$$
\begin{aligned}
E_{es,i,s,h} = & E_{es,i,s,h-1} + \eta^{ch}_{es} P^{ch}_{es,i,s,h} \\
& - \beta^{dch}_{es} P^{dch}_{es,i,s,h} \text{ where } \beta^{dch}_{es} = \frac{1}{\eta^{dch}_{es}}
\end{aligned} \tag{19}
$$

$$
E^{min}_{es,i,s,h} u_{es,i,h} \leq E_{es,i,s,h} \leq E^{max}_{es,i,s,h} u_{es,i,h} \tag{20}
$$

$$
E_{es,i,s,h_0} = \mu_{es} u_{es,i,h} E^{max}_{es,i} \tag{21}
$$

$$
E_{es,i,s,h_f} = E_{es,i,s,h_0} \tag{22}
$$

The charging and discharging limits related to ESS are depicted in (16) and (17), respectively. Note that $u_{es,i,h}$ is a control variable, set to 1 in this study, that defines if a storage unit is connected or not. Constraint (18) ensures that charging and discharging cannot occur simultaneously. The amount of energy available in ESS at hour *h* depends on the state of charge at the previous hour and on the charge or discharge cycle, on hour *h*, as demonstrated in (19). The maximum and

minimum storage capacity at hour *h* are also considered in (20). Constraints (21) and (22) ensure that there is an initial charge storage level (21), and that at the end of the cycle (h_f) the amount of energy stored is the same as the initial ESS level (22). These constraints ensure that the obtained solution does not depend on the initial reservoir level.

Charging and discharging inefficiencies are considered in order to model losses (electrical, chemical, etc.). In this study, charging and discharging efficiencies are considered equal.

Active and reactive power limits related to DGs are presented below:

$$0 \leq P_{g,i,s,h} \leq P^{max}_{g,i,s,h} \tag{23}$$

$$0 \leq Q_{g,i,s,h} \leq Q^{max}_{g,i,s,h} \tag{24}$$

In the case of variable generation sources, $P^{max}_{g,i,s,h}$ should be equal to the actual production at a specific hour. In this study, wind and solar (PV) type DGs are considered to have reactive power support capabilities. To model this, the following constraint must be considered:

$$-\tan(\cos^{-1}(pf_g)) * P_{g,i,s,h} \leq Q_{g,i,s,h} \tag{25}$$

$$Q_{g,i,s,h} \leq \tan(\cos^{-1}(pf_g)) * P_{g,i,s,h} \tag{26}$$

In (25) and (26) it can be observed that, DGs are capable of operating between a leading and lagging power factor.

The reactive power at the substation is constrained as:

$$Q^{SS,\,min}_{\zeta,s,h} \leq Q^{SS}_{\zeta,s,h} \leq Q^{SS,\,max}_{\zeta,s,h} \tag{27}$$

where the minimum and maximum reactive power limits could be calculated as in (28) and (29):

$$Q^{SS,\,max}_{\zeta,s,h} = \tan(\cos^{-1}(pf_{ss})) * P^{SS}_{\zeta,s,h} \tag{28}$$

$$Q^{SS,\,min}_{\zeta,s,h} = -\tan(\cos^{-1}(pf_{ss})) * P^{SS}_{\zeta,s,h} \tag{29}$$

The following constraint related to capacitor banks ensures the reactive power produced is bounded between zero and the maximum capacity:

$$0 \leq Q^{cb}_{i,s,h} \leq Q^{cb,\,max}_{i} \tag{30}$$

III. Case Study, Results and Discussion

A. System Data and Assumptions

Information regarding the radial network used to test the proposed operation model, can be found in [16]. For the base case, no lower voltage restrictions were considered, and the presented results correspond to a substation power factor of 0.8. This power factor, despite unrealistic, was chosen to ensure that, on the base case, all of the reactive demand was met. Note that for the base case, all DGs, SCBs and ESSs are not connected. This way, the only available power comes from the upstream grid, which would mean that there would be unserved reactive demand for high power factors. To ease the analysis of different cases and scenarios, the minimum power factor at the substation level was maintained at 0.8.

The location of capacitor banks, energy storage systems and DGs can also be found in [16], with the only change on the installed wind capacity on bus 14 which is now 2 MW instead of 3 MW. This change was made in order to better evaluate the impact of ESS in coping with the variability of RES. In this study, as mentioned in II-B, DGs are considered to have a reactive power support with a power factor of 0.95.

In addition, the following assumptions were made when carrying out the simulations:

- A 24 hour period was considered.
- Electricity price follows the same trend as demand.
- Nominal voltage is 12.66 kV.
- $\Delta V^{min} = -5\% * V_{nom}$ and $\Delta V^{max} = 5\% * V_{nom}$.
- The number of partitions (*Y*) is set equal to 5.
- $\eta^{ch}_{es} = 90\%$, unless otherwise mentioned.
- $ER_{SS} = 0.4\ tCO_2e/MWh$.
- Emission rate of DGs is set to 0.0276 and 0.0584 tCO_2e/MWh for wind and solar, respectively.
- $\lambda^{CO2}_{s,h} = 6$ €/tCO_2e.
- Electricity tariffs of wind and solar power generators are 20 and 40 €/MWh, respectively.
- $\lambda^{dch}_{s,h} = 5$ €/MWh.
- At node 1, $V_1 = V_{nom}$ and $\theta_1 = 0$.
- $v_{s,h} = 3000$ €/MW.

This study considers the combination of ten different scenarios for representing uncertainty related to demand, wind and solar power outputs, leading to a total of 1000 scenarios.

B. Results and Discussions

In order to analyze the behavior and impact of DGs, ESS and SCBs on the system, several cases were considered:

- Base case: Only importing power from the upstream grid is considered, while DGs, ESSs and SCBs are not connected.
- CB only: Only SCBs are connected, while DGs and ESSs are not.
- Efficiency (EFF) 0.9: DGs, ESSs and SCBs are connected. Storage efficiency set to 90%.
- EFF 0.8: The same as case "EFF 0.9", but ESS efficiency was reduced to 80%.
- EFF 0.7: The same as case "EFF 0.9", but ESS efficiency was reduced to 70%.
- Lim Q: The same as case "EFF 0.9", but constraints related to reactive power were not considered.

For each case, other than the "Lim Q" one, reactive power constraints were considered. The purpose of removing these constraints for the last case was to observe the behavior of the system when power export was allowed.

Voltage profiles for all cases can be seen in Fig. 1. It can be observed that for the base case, voltage deviations surpassed the minimum limit due to the high reactive power requirement in the system. To avoid infeasibility, in addition to lowering the power factor of the substation to 0.8, there was a need to remove the minimum voltage deviation constraints, only for the base case.

Emissions and import costs for each case, as well as the corresponding average losses are presented in Table I.

As expected, for the base case, where only import is considered, voltage deviations increased throughout the system

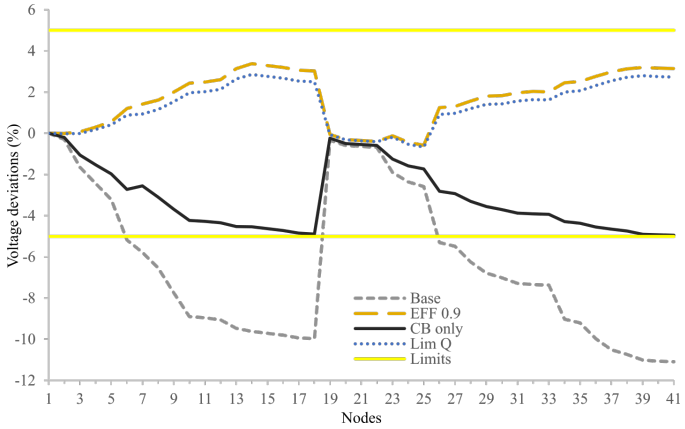

Fig. 1. Average voltage deviations at each node for each case

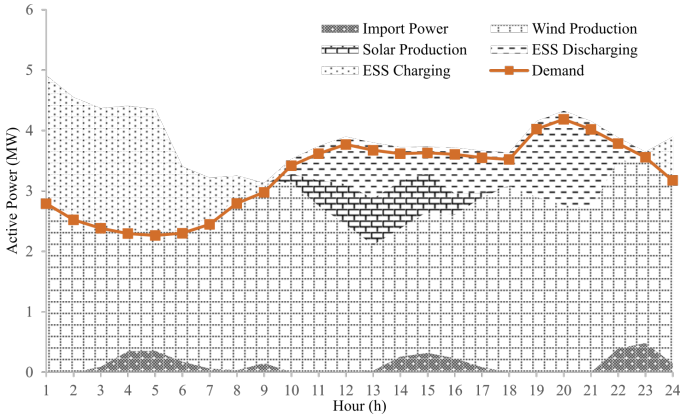

Fig. 2. Energy mix for Case: EFF 0.9

TABLE I
RELEVANT SYSTEM VARIABLES FOR EACH CASE

Case	Base	CB only	EFF 0.9	EFF 0.8	EFF 0.7	Lim Q
Operation Cost (€)						
DG	0	0	1667.83	1699.13	1724.28	1788.28
ESS	0	0	52.84	43.25	29.08	67.87
Cost of Import (€)	5999.8	5842.75	180.65	267.27	364.29	-214.14
Cost of Emissions (€)						
DG	0	0	13.88	14.15	14.38	14.92
Substation	205.87	200.34	7.67	10.33	12.62	2.66
Total Cost (€)	6205.67	6043.09	1922.87	2034.13	2144.65	1659.58
Average Losses						
PL (MW)	0.33	0.23	0.1	0.09	0.09	0.15
QL (MVAr)	0.23	0.17	0.08	0.08	0.07	0.11

especially for buses on the far end. Furthermore, as bus 1 is considered to have a deviation of 0%, then all downstream buses will have a negative voltage deviation, as power flows from upstream to downstream, a classic system power flow. Note that profiles shown above represent averages. The voltage deviation, for the base case, at bus 41 could vary between -7.7% and -14.3% for low and high demand scenarios, respectively. In the matter of cost in this case, there is a high cost of imported energy and the respective emission cost. Moreover, this case presents the highest value of both active and reactive power losses.

With the inclusion of capacitor banks (Case CB only), voltage deviation could be managed since there are now reactive power sources within the system. Voltage profiles now respect the limits as it can be seen in Fig. 1. By including capacitor banks, losses have decreased (Table I), as expected, which in turn affected the imported power, reducing the amount of both active and reactive power required from the substation. Including reactive power sources reduced cost by 2.6%, and more importantly, voltage deviations improved on average by 45.1% respecting the imposed limits. Since in this case only the upstream grid and SCBs were considered, costs only concern imported power and its respective emissions, as in the first case. In addition, this case also follows the classic grid active power flow.

Considering all technologies connected to the grid (DGs, ESSs and SCBs) there is a complete change on the voltage profile, as seen in Fig. 1, for all remaining cases. As DGs were included, voltage profiles were altered so that power flows can now occur from downstream to upstream. For example, bus 14, 32 and 38 have the highest installed capacity of DGs, and each one of these buses belongs to a different branch of the grid, and are located near the end of the corresponding branch. As it can be observed in Fig. 1, bus 14 and 32 have the highest positive deviation (of the corresponding branch), which means they dispatch energy for the surrounding buses and loads, because production surpasses the local demand. As for bus 38, it has another bus with DGs in the same branch (bus 39), it dispatches power to upstream buses since demand at node 39, 40 and 41 are met by the local production at bus 39. Note that the situation at bus 38 only occurs because local production at bus 39 surpasses local demand.

The energy mix for the case where DGs, ESSs and SCBs are connected to the system can be analyzed in Fig. 2. It can be observed that during valley hours, the system uses the excess wind power production and a slight import of power, since prices are low, to charge the energy storage systems. When wind power production diminishes, ESSs begin to discharge and together with solar production the demand is met. Because solar power production is more expensive, regarding tariffs, than ESSs and wind power production, we observed a curtailment of solar power since discharging the stored energy was cheaper, because it originated from wind type DGs. Despite being more expensive, solar PVs must be used, since later in the day, there will not be any and power import will be more expensive. In other words, a total curtailment of solar power would be counterproductive since ESSs can be used more efficiently later in the day, and also because it would mean curtailing a valuable resource totally dependent on the time of day. In order to compensate the lack of solar power during peak hours, when electricity prices are higher, ESSs can be used to partially meet demand, avoiding the need to import energy at high prices.

The difference in the actual power production and demand profiles (visible during peak hours) is because of losses in the system.

Considering ESSs with lower efficiencies leads to a decrease in the utilization of these systems, since it would require more energy to use them efficiently. When ESS efficiency is reduced, the otherwise curtailed solar production must now be used to compensate. In Table I, both cases with altered efficiencies presented a higher cost of operation and emissions of DGs, because of increased use of solar power, and at the same time more import power cost, and respective emissions, since stored energy was intended to be used later in the day when electricity price is higher. On the other hand, losses decreased slightly when compared to Case: EFF 0.9 since less discharge power was used. Moreover, voltage profiles did not change significantly for different ESS efficiencies (i.e cases EFF 0.8 and EFF 0.7) when compared to the profile in case EFF 0.9.

When excluding the reactive power limits, export is now allowed, which means import prices can be negative (excess power can be sold to the grid), reducing the objective function. This is proved by the fact that this case presents the lowest cost, as demonstrated in Table I. Losses increase because DG nodes are on the far end of the grid and in order to export active power, it must pass through several lines until it reaches the substation, increasing losses (when compared with Case: EFF 0.9). However, they are still less than in the Base case. Voltage profiles are slightly improved when compared to EFF 0.9 case, since there is active power export at the same time as reactive power import.

IV. Conclusion

This work proposed a new stochastic MILP model that aims to ensure a more efficient utilization of variable renewables at distribution levels. The results show that the integration of ESS together with reactive power sources could cope with the variability of RES, reducing losses and cost, while improving voltage profiles.

Because of ESS, renewable energy penetration increased significantly, since excess wind power could be stored and used later, instead of being curtailed. This way, the integration of ESS allows a more efficient use of renewable energy sources, which are almost emission-free power source, and this is reflected in the cost. In fact, RESs can represent 96% of the total power production. A good planning of the location and capacity of RES is also required, since this will affect losses and depending on the locations, sizes as well as the profile of wind and solar outputs. As demonstrated in this study, with the integration of RESs, ESSs and SCBs in the right locations, active power losses in the EFF 0.9 case could be reduced by 70% on average, and total cost in the same case by 69%. Furthermore, the proposed model considerably improves voltage profiles in the system, which in turn contributes to an increased voltage stability margin which is essential for a secure operation of the system.

References

[1] B. Muruganantham, R. Gnanadass, and N. Padhy, "Challenges with renewable energy sources and storage in practical distribution systems," Renewable and Sustainable Energy Reviews, vol. 73, pp. 125–134, June 2017.

[2] S. Nandi, P. Biswas, V. N. Nandakumar, and R. K. Hedge, "Two novel schemes suitable for static switching of three-phase delta-connected capacitor banks with minimum surge current," IEEE Transactions on Industry Applications, vol. 33, no. 5, pp. 1348–1354, 1997.

[3] H. Nosair and F. Bouffard, "Flexibility Envelopes for Power System Operational Planning," IEEE Transactions on Sustainable Energy, vol. 6, pp. 800–809, July 2015.

[4] W. A. Bukhsh, C. Zhang, and P. Pinson, "An Integrated Multiperiod OPF Model With Demand Response and Renewable Generation Uncertainty," IEEE Transactions on Smart Grid, vol. 7, pp. 1495–1503, May 2016.

[5] M. Masoum, A. Jafarian, M. Ladjevardi, E. Fuchs, and W. Grady, "Fuzzy Approach for Optimal Placement and Sizing of Capacitor Banks in the Presence of Harmonics," IEEE Transactions on Power Delivery, vol. 19, pp. 822–829, Apr. 2004.

[6] B. Zakeri and S. Syri, "Electrical energy storage systems: A comparative life cycle cost analysis," Renewable and Sustainable Energy Reviews, vol. 42, pp. 569–596, Feb. 2015.

[7] A. Colmenar-Santos, C. Reino-Rio, D. Borge-Diez, and E. Collado-Fernández, "Distributed generation: A review of factors that can contribute most to achieve a scenario of DG units embedded in the new distribution networks," Renewable and Sustainable Energy Reviews, vol. 59, pp. 1130–1148, June 2016.

[8] P. Poonpun and W. Jewell, "Analysis of the Cost per Kilowatt Hour to Store Electricity," IEEE Transactions on Energy Conversion, vol. 23, pp. 529–534, June 2008.

[9] M. H. Tushar and C. Assi, "Volt-VAR Control through Joint Optimization of Capacitor Bank Switching, Renewable Energy, and Home Appliances," IEEE Transactions on Smart Grid, pp. 1–1, 2017.

[10] S. Soto and V. Hinojosa, "Stochastic optimal allocation of reactive power banks for system loss minimization," IEEE Latin America Transactions, vol. 14, no. 4, pp. 1980–1987, 2016.

[11] K. Hur and S. Santoso, "Distance Estimation of Switched Capacitor Banks in Utility Distribution Feeders," IEEE Transactions on Power Delivery, vol. 22, pp. 2419–2427, Oct. 2007.

[12] S. Santoso, "On Determining the Relative Location of Switched Capacitor Banks," IEEE Transactions on Power Delivery, vol. 22, pp. 1108–1116, Apr. 2007.

[13] R. Jabr, "Optimal placement of capacitors in a radial network using conic and mixed integer linear programming," Electric Power Systems Research, vol. 78, pp. 941–948, June 2008.

[14] S. Segura, R. Romero, and M. J. Rider, "Efficient heuristic algorithm used for optimal capacitor placement in distribution systems," International Journal of Electrical Power & Energy Systems, vol. 32, pp. 71–78, Jan. 2010.

[15] H. Khani, M. Moallem, S. Sadri, and M. Dolatshahi, "A New Method for Online Determination of the Location of Switched Capacitor Banks in Distribution Systems," IEEE Transactions on Power Delivery, vol. 26, pp. 341–351, Jan. 2011.

[16] S. F. Santos, D. Z. Fitiwi, M. Shafie-khah, A. W. Bizuayehu, C. M. P. Cabrita, and J. P. S. Catalao, "New multi-stage and stochastic mathematical model for maximizing RES hosting capacity—part II: Numerical results," vol. 8, no. 1, pp. 320–330.

[17] S. F. Santos, D. Z. Fitiwi, M. Shafie-Khah, A. W. Bizuayehu, C. M. P. Cabrita, and J. P. S. Catalao, "New multistage and stochastic mathematical model for maximizing RES hosting capacity—part I: Problem formulation," vol. 8, no. 1, pp. 304–319.

[18] D. Z. Fitiwi, L. Olmos, M. Rivier, F. de Cuadra, and I. Pérez-Arriaga, "Finding a representative network losses model for large-scale transmission expansion planning with renewable energy sources," vol. 101, pp. 343–358.

[19] J. P. Vielma, S. Ahmed, and G. Nemhauser, "Mixed-Integer Models for Nonseparable Piecewise-Linear Optimization: Unifying Framework and Extensions," Operations Research, vol. 58, pp. 303–315, Apr. 2010.